

**SPACE WEATHERING EFFECTS IN LUNAR SOILS: THE ROLES OF SURFACE EXPOSURE TIME AND BULK CHEMICAL COMPOSITION.** Shouliang Zhang<sup>1</sup> and Lindsay P. Keller<sup>2</sup>, <sup>1</sup>Lunar and Planetary Institute, 3600 Bay Area Blvd., Houston, TX 77058 and <sup>2</sup>ARES, Mail Code KR, NASA Johnson Space Center, Houston, TX 77058, [zhang@lpi.usra.edu](mailto:zhang@lpi.usra.edu)

**Introduction:** Space weathering effects on lunar soil grains result from both radiation-damaged and deposited layers on grain surfaces. Typically, solar wind irradiation forms an amorphous layer on regolith silicate grains, and induces the formation of surficial metallic Fe in Fe-bearing minerals [1,2]. Impacts into the lunar regolith generate high temperature melts and vapor. The vapor component is largely deposited on the surfaces of lunar soil grains [3] as is a fraction of the melt [4, this work]. Both the vapor-deposits and the deposited melt typically contain nanophase Fe metal particles (npFe<sup>0</sup>) as abundant inclusions. The development of these rims and the abundance of the npFe<sup>0</sup> in lunar regolith, and thus the optical properties, vary with the soil mineralogy and the length of time the soil grains have been exposed to space weathering effects [5]. In this study, we used the density of solar flare particle tracks in soil grains to estimate exposure times for individual grains and then perform nanometer-scale characterization of the rims using transmission electron microscopy (TEM). The work involved study of lunar soil samples with different mineralogy (mare vs. highland) and different exposure times (mature vs. immature).

**Materials and experimental methods:** Aliquots of the <20 μm fraction of mare soils 10084 (I<sub>s</sub>/FeO ~78, mature), and 71061 (I<sub>s</sub>/FeO ~14, immature), and a highland soil 72051 (I<sub>s</sub>/FeO ~81, mature), were embedded in low viscosity epoxy, and thin sections were prepared using ultramicrotomy. Numerous mineral grains in the thin sections from each sample site were randomly selected and analyzed using the JSC JEOL 2500SE 200kV field-emission, scanning and transmission electron microscopy (STEM) equipped with a Noran ultra-thin window energy-dispersive x-ray (EDX) spectrometer detector and a Tridiem Gatan Image Filter (GIF).

**Results and discussion:** In the <20 μm 10084 sample nearly all mineral grains are surrounded with space weathered rims, either irradiation, deposition or occasionally both with multiple layers [3, this study]. The average total rim thickness is ~50 nm in 10084 with large grain-to-grain variation, ranging from less than 10 nm up to ~200 nm. Solar wind irradiation and melt/vapor deposition have comparable contributions to the formation of rims in 10084 [3]. In the immature sample 71061, only ~10% of the mineral grains have rims and most of these were formed through depositional processes. For example, rims on anorthite grains

contain abundant npFe<sup>0</sup> particles and show little evidence of irradiation processing.

We studied the evolution of rims with exposure time by correlating the rim thickness and composition with the solar flare particle track density registered on the substrate from grain to grain at the nm-scale. The track density was estimated by counting the number of tracks in 100 nm × 100 nm areas in dark-field TEM images (Figure 1) and then converting this to n<sub>SFT</sub>/cm<sup>2</sup> (where n<sub>SFT</sub> is the # of solar flare tracks). The results show that the thickness of the irradiation-induced rims is positively correlated with the exposure time and can increase up to 100 nm with the highest observed track density ~3×10<sup>11</sup> n<sub>SFT</sub>/cm<sup>2</sup> (Figure 2), but the average thickness of most rims is ~50 nm with an average track density of ~1-1.5×10<sup>11</sup> n<sub>SFT</sub>/cm<sup>2</sup>. In the deposited rims, however, the thickness is highly variable (10-200 nm) and interestingly, is largely independent of the exposure time based on track densities. This observation suggests that the formation of vapor-deposited rims is not a gradual process with the accumulation of greater thicknesses of material over time, but instead, that the bulk of the rim material is deposited in only a few events or possibly a single event. This time correlation also indicates that deposition process is dominant over irradiation at the initial stage of space weathering, which is consistent with the observations from the immature sample (71061). With longer exposure time, the irradiation induced layer increases until reaching a “saturated” thickness, in accordance to the penetration depth of solar wind ions (e.g. proton, helium ion) in the mineral grains. These results are broadly consistent with our numerical modeling of rim thicknesses as a function of exposure time [6]. Meanwhile, increasing number of soil grains received contribution from melt/vapor deposition. For each individual grain, however, the deposition-formed rim is not necessarily accumulated over time.

We investigated the effect of bulk chemical composition on the formation of space weathered rims by analyzing grains in two mature samples, 10084 (mare) and 72051 (highland). Among 50 grains randomly selected from each TEM grid for analysis thus far, the average thickness of the irradiation-induced rims is similar, ~50 nm, while there is noticeably different contribution from melt/vapor deposition as well as chemical and textural differences in the deposited rims between these two samples. In 10084, almost 80% of grains are covered by the melt or vapor-deposited ma-

terials with or without an irradiated layer. In contrast, only 50% of grains exhibit deposited rims in 72051. For comparison, more than 90% of grains from 72501 bear irradiated layer. The abundance of deposited rims in the mature mare soil compared to the mature highland soil is likely related to the different melting and vaporization temperatures for these materials. Regardless of the mineral substrate, an Al-rich layer (~50 nm) without inclusions of  $\text{npFe}^0$  particles is commonly found as the rim component (Figure 3). The  $\text{npFe}^0$  inclusions are more abundant in the deposited rims on soil grains from mature mare soils than mature highland soils and is likely related to differences in bulk Fe abundance [7]. In summary, the reduced amount of melt/vapor deposition and less abundant  $\text{npFe}^0$  in both the deposition- and irradiation-formed rims in highland 72051 soil could modify optical properties from those of mare 10084 soil, even though they have similar maturity index.

**References:** [1] Zhang, S. and Keller, L. P. (2010) *LPSC 41st*, #1432. [2] Christoffersen, R. et al. (1996) *Meteoritics & Planet. Sci.* 31, 835-848. [3] Keller, L. P. and McKay, D. S. (1997) *Geochim. Cosmochim. Acta.* 61, 2331-2341. [4] Noble, S. K. et al. (2007) *LPS XXXVIII*, #1359. [5] Pieters, C. M. et al. (1993) *J. Geophys. Res.* 98, 20817-20824. [6] Chamberlin, S. et al. (2008) *LPS XXXIX*, #2302. [7] Noble, S. K. et al. (2001) *Meteoritics & Planet. Sci.* 36, 31-42.

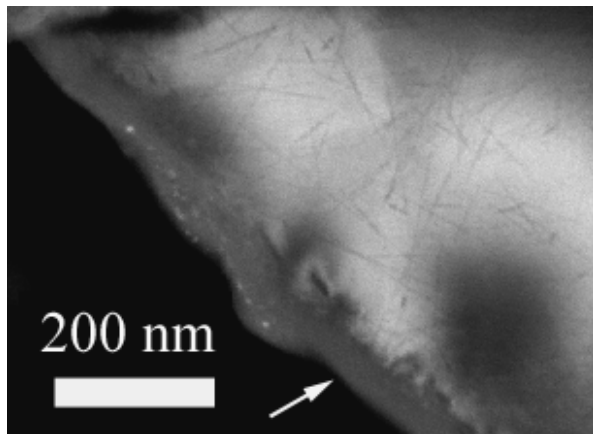


Figure 1. STEM dark field image of an anorthite grain with 40 nm irradiation-induced amorphous layer (arrow marker). The solar flare track density is estimated as  $8 \times 10^{10}/\text{cm}^2$ .

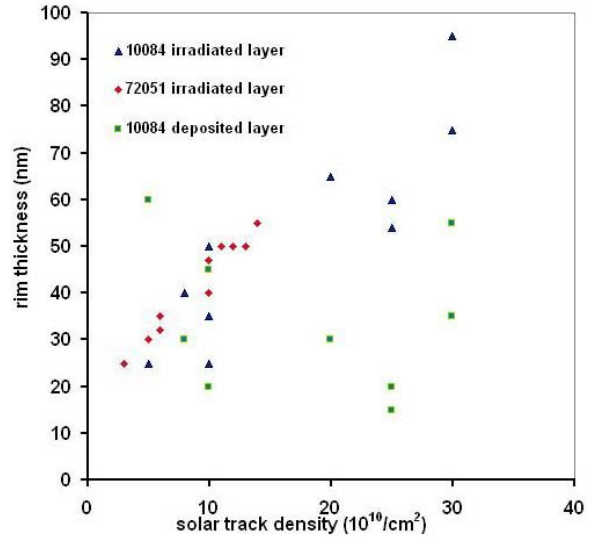


Figure 2. plot of the correlation between solar track density and different types of rims from mare (10084) and highland site (72051).

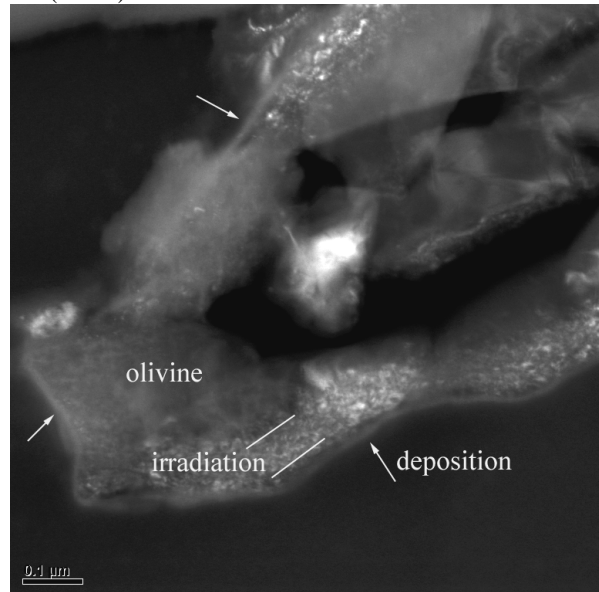


Figure 3. STEM dark field image of an olivine grain with irradiation-damaged layer overlain by the deposition-formed, Al-rich rim. Such type of rim is commonly found in highland 72051 sample.